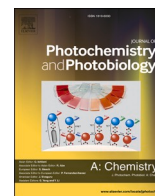




Contents lists available at ScienceDirect

## Journal of Photochemistry &amp; Photobiology, A: Chemistry

journal homepage: [www.elsevier.com/locate/jphotochem](http://www.elsevier.com/locate/jphotochem)

# A novel fluorescent probe based on 7,8-benzochromone-3-carbaldehyde-(rhodamine B carbonyl) hydrazone for detection of trivalent cations and $Zn^{2+}$ in different systems

Jie Sun, Tian-rong Li\*, Zheng-yin Yang\*

College of Chemistry and Chemical Engineering, State Key Laboratory of Applied Organic Chemistry, Lanzhou University, Lanzhou, 730000, PR China

## ARTICLE INFO

## Keywords:

Benzochromone  
Rhodamine B  
Fluorescence probe  
Trivalent cation  
 $Zn^{2+}$

## ABSTRACT

In this article, a new fluorescence probe 7,8-benzochromone-3-carbaldehyde-(rhodamine B carbonyl) hydrazone (L) was synthesized, which had been explored to detect  $Zn^{2+}$  and trivalent metal ions  $M^{3+}$  ( $Al^{3+}$ ,  $Cr^{3+}$  and  $Fe^{3+}$ ). When the excitation wavelength was 490 nm, L showed high selectivity and high sensitivity to  $M^{3+}$  which was superior to monovalent and divalent metal cations in methanol solution. In EtOH/H<sub>2</sub>O (15/1, V/V), L showed selective fluorescence response to  $Zn^{2+}$ , when the excitation wavelength was set to 425 nm. Furthermore, the detection limits of L for  $Fe^{3+}$ ,  $Al^{3+}$  and  $Cr^{3+}$  were  $2.46 \times 10^{-9}$  M,  $2.54 \times 10^{-9}$  M and  $4.23 \times 10^{-8}$  M, respectively. And the detection limit of L for  $Zn^{2+}$  was calculated to be  $1.45 \times 10^{-7}$  M. The coordination ratio between L and  $M^{3+}$  was determined from the Job's plot (fluorescent spectrum) to be 2:1 and the coordination ratio of L and  $Zn^{2+}$  was 1:1. Additionally, L might be used as a colorimetric probe of  $Cu^{2+}$  in EtOH/H<sub>2</sub>O (15/1, V/V) solution, which could be observed with the naked eye from colorless to red in the presence of  $Cu^{2+}$ .

## 1. Introduction

The synthesis of new fluorescent probes for detecting trivalent ions ( $M^{3+}=Fe^{3+}$ ,  $Al^{3+}$ ,  $Cr^{3+}$ ) is a topic worthy of research. Fluorescent probes have been widely used in the detection of metal cations, anions, and biomolecules due to their simple design, short response time, high selectivity, sensitivity and low detection limit [1–6]. The detection of trivalent metal ions is of great value due to their own environmental importance and biological significance. For example, Chromium is widely used in metal processing, electroplating, tanning and other industries. Waste water and waste gas containing a large amount of chromium produced in the industrial production process will be discharged into the environment [7,8]. When there is too much chromium in the soil, it will inhibit the nitrification of organic matter and cause chromium to accumulate in plants. Chromium in water bodies is lethal to aquatic organisms [9]. Simultaneously,  $Cr^{3+}$  is an essential element for human nutrition.  $Cr^{3+}$  can affect the body's lipid metabolism and reduce blood cholesterol and triglycerides [10,11]. However, the high content of  $Cr^{3+}$  in the organism not only negatively affects the cell structure, but even increases the risk of cardiovascular and cerebrovascular diseases and diabetes [11–15]. As we all know,  $Al^{3+}$ , as the third most abundant metal element in the earth's crust, is widely used in

the chemical industry, medical equipment, aircraft and ship manufacturing industries. However, the existence of a large amount of aluminum in nature can also cause environmental pollution and water resources damage. At the same time, the excessive content of  $Al^{3+}$  in the organism will cause the decline of liver and kidney function and interfere with the metabolism of  $Ca^{2+}$  [16–20]. In recent years, with the widespread application of iron in industrial production, a large amount of iron-containing waste water and waste gas are discharged into the environment, and they will gradually accumulate and enrich in the environment, causing serious pollution to the atmosphere, soil and water bodies [21]. Iron is an essential trace element for the human body. It has the function of participating in the transportation and storage of oxygen and enhancing resistance to diseases [22–25]. However, excessive intake of iron preparations may also lead to iron poisoning, causing liver cirrhosis and diabetes [26–29]. In addition, if the iron content in the water exceeds the standard, it will affect the sensory properties such as water color, smell and taste. Therefore, it is necessary to monitor the content of trivalent ions in the environment and some probes for detecting trivalent metal ions have been reported in the previous literature [10,30,31].

The probe synthesized in this article can not only detect  $M^{3+}$  in methanol but also detect  $Zn^{2+}$  in EtOH/H<sub>2</sub>O (15/1, V/V). Zinc is one of

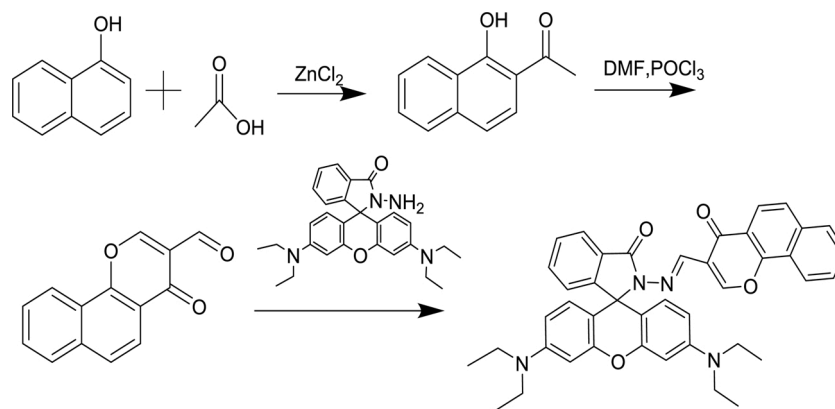
\* Corresponding authors.

E-mail addresses: [litr@lzu.edu.cn](mailto:litr@lzu.edu.cn) (T.-r. Li), [yangzy@lzu.edu.cn](mailto:yangzy@lzu.edu.cn) (Z.-y. Yang).<https://doi.org/10.1016/j.jphotochem.2021.113207>

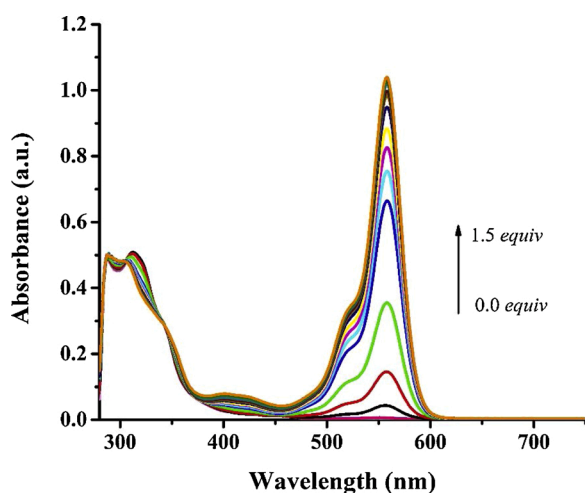
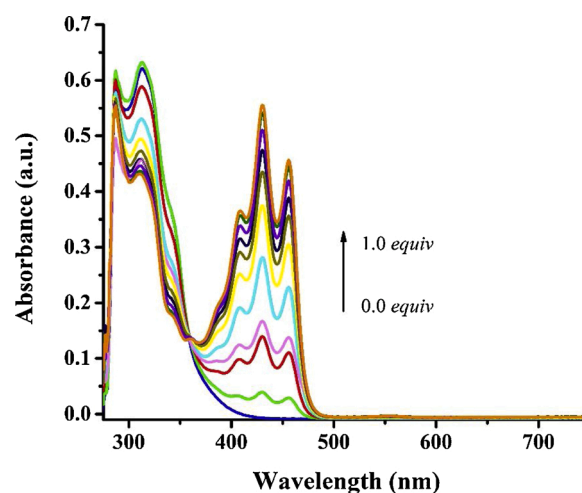
Received 29 November 2020; Received in revised form 8 February 2021; Accepted 9 February 2021

Available online 15 February 2021

1010-6030/© 2021 Elsevier B.V. All rights reserved.



Scheme 1. Synthetic route of L.

Fig. 1. The UV-vis absorption titration spectrum of L (25  $\mu\text{M}$ ) with  $\text{Al}^{3+}$  (0.0–1.5 equiv) in methanol.Fig. 2. The UV-vis absorption titration spectrum of L (25  $\mu\text{M}$ ) with  $\text{Zn}^{2+}$  (0.0–1.0 equiv) in EtOH/ $\text{H}_2\text{O}$  (15/1, V/V).

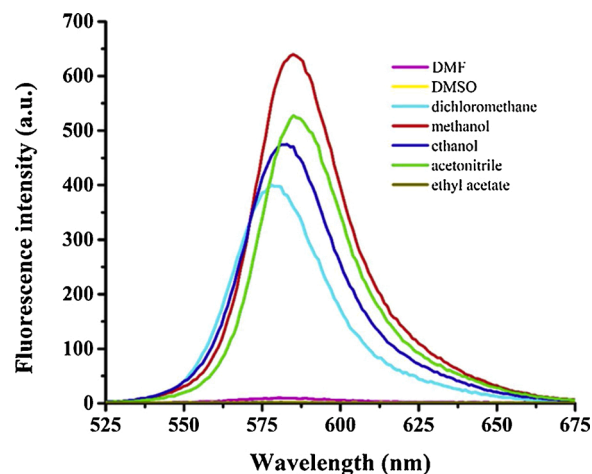
the 25 essential elements in the human body. The imbalance of zinc content in the human body can lead to diseases such as digestive disorders and low immunity [32–34]. At the same time, with the widespread application of zinc in the battery, construction, and shipbuilding industries, there is a large amount of zinc in the environment, causing serious pollution and affecting plant growth [35,36]. Therefore, highly selective detection of zinc ions is worth achieving. In EtOH/ $\text{H}_2\text{O}$  (15/1, V/V) solution, L showed superior fluorescence selectivity to  $\text{Zn}^{2+}$  than other metal ions. Interestingly, in the EtOH/ $\text{H}_2\text{O}$  (15/1, V/V) solution, the addition of  $\text{Cu}^{2+}$  to L showed a red color different from that of L added with other metal ions, indicating that the colorimetry of  $\text{Cu}^{2+}$  can be detected in this solution. Herein, the optical properties of L to  $\text{M}^{3+}$  and  $\text{Zn}^{2+}$  were studied through fluorescence spectra, IR spectra and UV-vis spectra, the colorimetric properties of L to  $\text{Cu}^{2+}$  through UV-vis spectra.

## 2. Experimental

### 2.1. Materials and instruments

1-Naphthol was provided by Shanghai Macklin Biochemical Co., Ltd. Rhodamine B was obtained from Tianjin Guangfu Fine Chemical Research Institute. All solvents were purchased from Li'an Long Bohua Tianjin Pharmaceutical Chemical Co., Ltd. All the above solvents and chemicals could be used without further purification.  $^1\text{H}$  NMR and  $^{13}\text{C}$  NMR spectra were obtained using a Bruker 400 MHz instruments with

TMS as an internal standard. IR spectra were obtained in KBr discs on a Thermo Mattson FT-IR spectrometer. High Resolution Mass Spectrometry (HRMS) was measured on Bruker esquire 6000 spectrometer. ESI-MS spectrum was recorded by Bruker esquire 6000 spectrometer. Fluorescence spectra and UV-vis absorption spectra were obtained using Hitachi RF-4500 spectrophotometer and Shimadzu UV-240

Fig. 3. Solvent effect on fluorescence intensity of the probe L with  $\text{Al}^{3+}$  in different solvent.

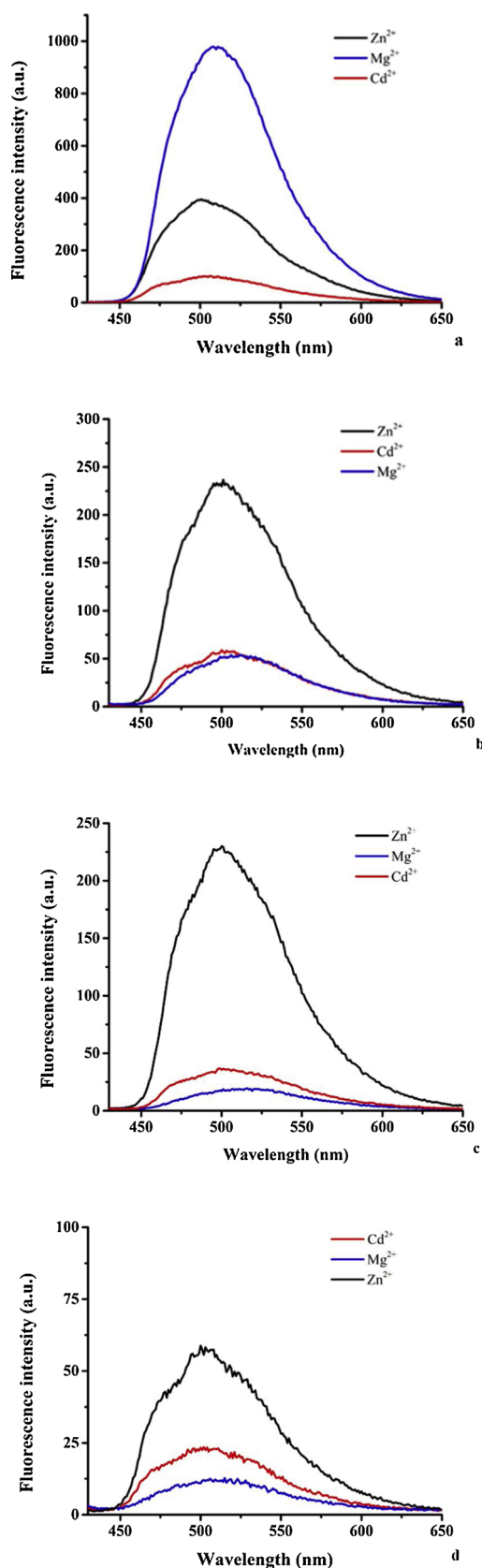


Fig. 4. Solvent effect on fluorescence intensity of the probe L with  $\text{Co}^{2+}$ ,  $\text{Mg}^{2+}$  and  $\text{Zn}^{2+}$  in solvent of different ratios of EtOH/ $\text{H}_2\text{O}$ : a) ethanol; b) EtOH/ $\text{H}_2\text{O}$  (20/1, V/V); c) EtOH/ $\text{H}_2\text{O}$  (15/1, V/V); d) EtOH/ $\text{H}_2\text{O}$  (10/1, V/V).

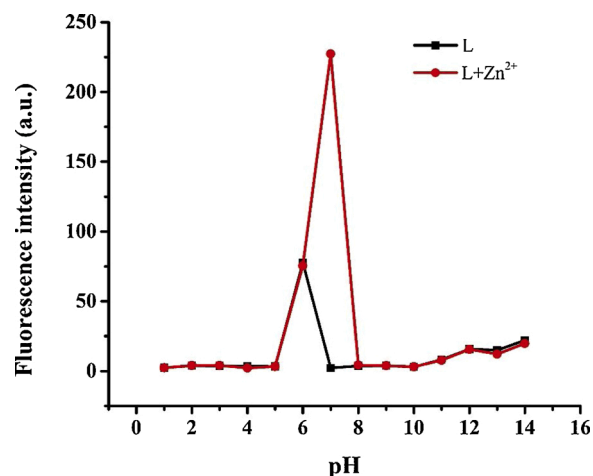


Fig. 5. Variation of fluorescence intensity of L (50 mM) in EtOH/ $\text{H}_2\text{O}$  (15/1, V/V) solution with and without  $\text{Zn}^{2+}$  (1.0 equiv.) as a function of pH.

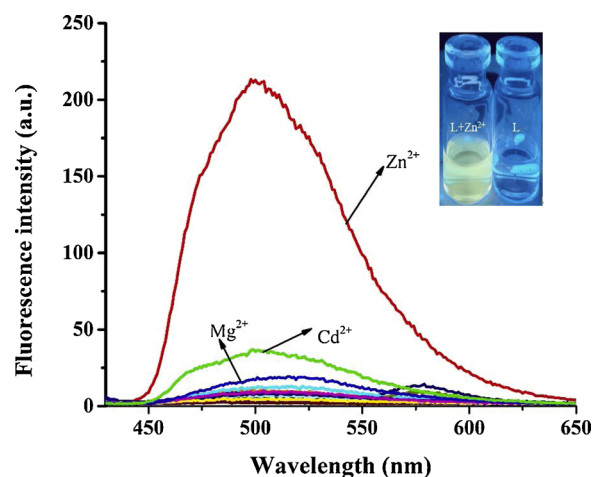


Fig. 6. Fluorescence spectra of L (25  $\mu\text{M}$ ) after addition of 1 equiv of various metal ions of  $\text{Li}^+$ ,  $\text{Ag}^+$ ,  $\text{Ca}^{2+}$ ,  $\text{Co}^{2+}$ ,  $\text{Cu}^{2+}$ ,  $\text{Fe}^{3+}$ ,  $\text{Mg}^{2+}$ ,  $\text{Na}^+$ ,  $\text{Pb}^{2+}$ ,  $\text{Ba}^{2+}$ ,  $\text{Cd}^{2+}$ ,  $\text{Cr}^{3+}$ ,  $\text{Fe}^{2+}$ ,  $\text{K}^+$ ,  $\text{Mn}^{2+}$ ,  $\text{Ni}^{2+}$ ,  $\text{Hg}^{2+}$ ,  $\text{Al}^{3+}$  and  $\text{Zn}^{2+}$  in EtOH/ $\text{H}_2\text{O}$  (15/1, V/V). Inset: fluorescence response of L in the presence of  $\text{Zn}^{2+}$  and L under 365 nm UV lamp.

spectrophotometer, respectively. And the melting point was measured by Beijing XT4–100x microscopic melting point apparatus.

## 2.2. Synthesis of L

4-oxo-4H-benzo[h]methylene-3-carbaldehyde [37] and rhodamine B hydrazide [38] were synthesized according to previous reports. To a solution of 4-oxo-4H-benzo[h]methylene-3-carbaldehyde (0.13 g, 0.59 mmol) in ethanol was added rhodamine B hydrazide (0.27 g, 0.59 mmol). The solution was refluxed and stirred at  $80^\circ\text{C}$  for 18 h with appearance of white precipitation. The mixture was cooled at room temperature filtered under reduced pressure to obtain crude product. Then the crude product was recrystallized in ethanol and dried in vacuum. After the above steps, 7,8-benzochromone-3-carbaldehyde-(rhodamine B carbonyl) hydrazone (L) was synthesized (Scheme 1). Yield :51.4 % (0.20 g), mp:  $246\text{--}247^\circ\text{C}$ .  $^1\text{H}$  NMR (400 MHz,  $\text{DMSO-}d_6$ , TMS) (Fig. S1):  $\delta$ (ppm): 8.85 (s, 1 H), 8.38 (s, 1 H), 8.32 (d, 1 H,  $J=8$  Hz), 7.99 (d, 1 H,  $J=8$  Hz), 7.89 (d, 1 H,  $J=8$  Hz), 7.84 (m, 2 H) 7.70 (m, 2 H) 7.56 (m, 2 H), 7.05 (d, 1 H,  $J=8$  Hz), 6.43 (d, 2 H,  $J=4$  Hz), 6.42 (s, 1 H), 6.39 (s, 1 H), 6.31 (d, 1 H,  $J=4$  Hz), 6.29 (d, 1 H,  $J=4$  Hz), 3.25 (m, 8 H), 1.03 (t, 12 H,  $J=8$  Hz).  $^{13}\text{C}$  NMR (400 MHz,  $\text{DMSO-}d_6$ , TMS) (Fig. S14):

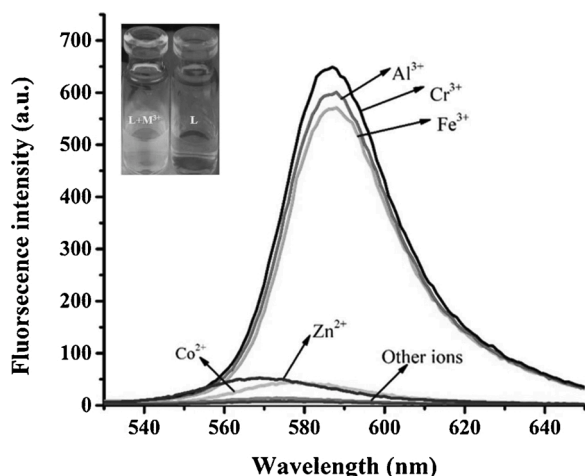


Fig. 7. Fluorescence spectra of L (25  $\mu\text{M}$ ) after addition of 1 equiv of various metal ions of  $\text{Li}^+$ ,  $\text{Ag}^+$ ,  $\text{Ca}^{2+}$ ,  $\text{Co}^{2+}$ ,  $\text{Cu}^{2+}$ ,  $\text{Fe}^{3+}$ ,  $\text{Mg}^{2+}$ ,  $\text{Na}^+$ ,  $\text{Pb}^{2+}$ ,  $\text{Ba}^{2+}$ ,  $\text{Cd}^{2+}$ ,  $\text{Cr}^{3+}$ ,  $\text{Fe}^{2+}$ ,  $\text{K}^+$ ,  $\text{Mn}^{2+}$ ,  $\text{Ni}^{2+}$ ,  $\text{Hg}^{2+}$ ,  $\text{Zn}^{2+}$  and  $\text{Al}^{3+}$  in methanol. Insert: fluorescence response of L in the presence of  $\text{M}^{3+}$  and L under 365 nm UV lamp.

$\delta$ (ppm): 174.77, 164.48, 153.33, 153.12, 152.00, 148.99, 140.15, 135.74, 134.54, 130.26, 129.27, 128.72, 128.63, 128.23, 128.02, 126.20, 124.29, 123.60, 122.30, 120.41, 120.37, 120.05, 108.52, 105.60, 97.94, 65.84, 56.50, 44.11, 19.04, 12.89. MS(ESI) (Fig. S3):  $m/z = 663.2163$   $[\text{M}+\text{H}]^+$ . HRMS (Fig. S13):  $m/z = 685.2781$   $[\text{M}+\text{Na}]^+$ ,  $m/z = 663.2965$   $[\text{M}+\text{H}]^+$ .

### 2.3. Measurement procedures

The 5 mM stock solution of various metal ions ( $\text{Na}^+$ ,  $\text{Mg}^{2+}$ ,  $\text{Ag}^+$ ,  $\text{K}^+$ ,  $\text{Li}^+$ ,  $\text{Hg}^{2+}$ ,  $\text{Cu}^{2+}$ ,  $\text{Zn}^{2+}$ ,  $\text{Ca}^{2+}$ ,  $\text{Co}^{2+}$ ,  $\text{Cd}^{2+}$ ,  $\text{Mn}^{2+}$ ,  $\text{Ba}^{2+}$ ,  $\text{Pb}^{2+}$ ,  $\text{Al}^{3+}$ ,  $\text{Cr}^{3+}$ ,  $\text{Fe}^{3+}$ ) were prepared in EtOH. All the metal ion solutions mentioned above were prepared from nitrate and chloride salts of metal ions. The 5 mM stock solution of L was obtained in DMF. Adding 2 mL of methanol solution or EtOH/ $\text{H}_2\text{O}$  (15/1, V/V) into a cuvette, and the stock solution of L (10  $\mu\text{L}$ ) and the stock solutions of various metal ion (1 equiv) were added into it to obtain the tested solution. In methanol solution, the excitation wavelength was set to 490 nm. The excitation and the emission slit were set to 3 nm and 3 nm, respectively. In EtOH/ $\text{H}_2\text{O}$  (15/1, V/V), the excitation wavelength was set to 425 nm. Both the excitation and the emission slit were set to 3 nm. All measurements were performed at atmospheric pressure and room temperature.

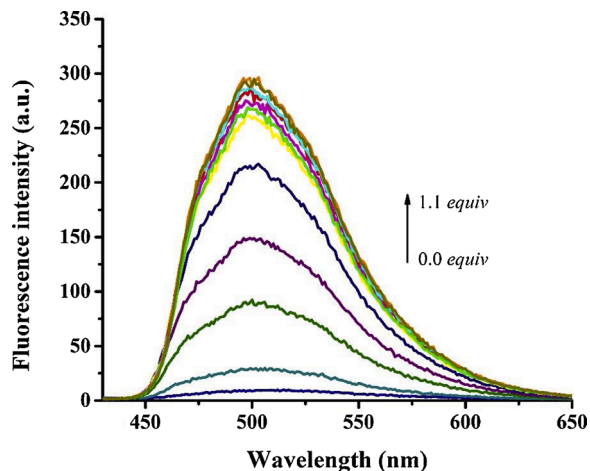
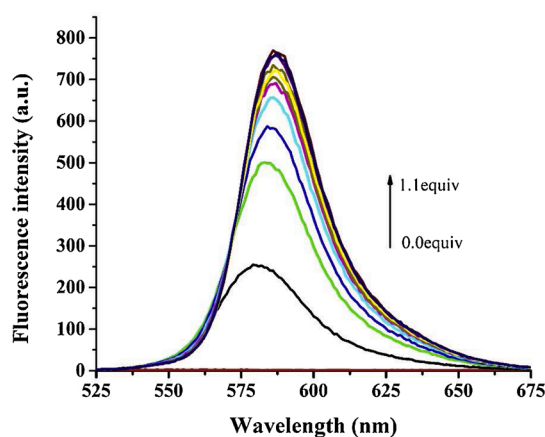
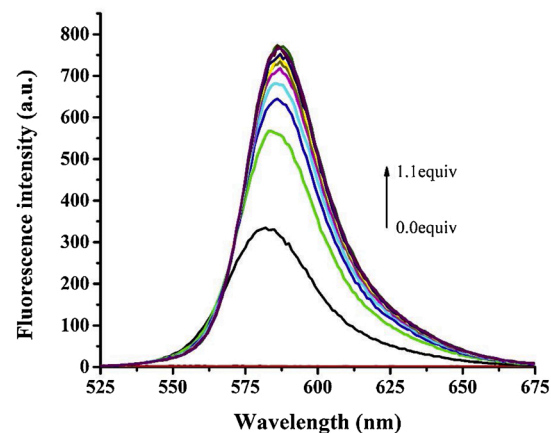


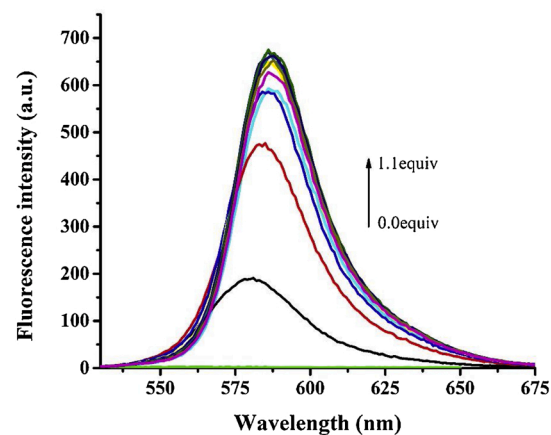
Fig. 8. Fluorescence emission titration spectra of L (25  $\mu\text{M}$ ) upon addition of  $\text{Zn}^{2+}$  (0.0–1.0 equiv) in EtOH/ $\text{H}_2\text{O}$  (15/1, V/V).



a



b



c

Fig. 9. a. Fluorescence emission titration spectra of L (25  $\mu\text{M}$ ) upon addition of  $\text{Al}^{3+}$  (0.0–1.0 equiv) in methanol. b. Fluorescence emission titration spectra of L (25  $\mu\text{M}$ ) upon addition of  $\text{Cr}^{3+}$  (0.0–1.0 equiv) in methanol. c. Fluorescence emission titration spectra of L (25  $\mu\text{M}$ ) upon addition of  $\text{Fe}^{3+}$  (0.0–1.0 equiv) in methanol.

## 3. Results and discuss

### 3.1. UV-vis studies of L towards $\text{M}^{3+}$ and L towards $\text{Zn}^{2+}$

The UV-vis studies of L to  $\text{M}^{3+}$  were conducted in methanol and the

**Table 1**  
Comparison of detection limit of Zn<sup>2+</sup> and M<sup>3+</sup> with other reported probes.

Solvent (V/V)	LOD/M				Reference
	Al <sup>3+</sup>	Cr <sup>3+</sup>	Fe <sup>3+</sup>	Zn <sup>2+</sup>	
CH <sub>3</sub> OH/H <sub>2</sub> O (6/4)	1.74 × 10 <sup>-9</sup>	2.36 × 10 <sup>-6</sup>	2.90 × 10 <sup>-6</sup>	/	[45]
CH <sub>3</sub> CN/HEPES buffer solution (40/60)	2.30 × 10 <sup>-5</sup>	2.50 × 10 <sup>-9</sup>	2.00 × 10 <sup>-5</sup>	/	[46]
methanol	6.90 × 10 <sup>-7</sup>	6.80 × 10 <sup>-5</sup>	6.50 × 10 <sup>-5</sup>	/	[47]
H <sub>2</sub> O/DMSO (9/1)	/	/	/	1.30 × 10 <sup>-7</sup>	[48]
DMF/H <sub>2</sub> O (1/1)	/	/	/	1.27 × 10 <sup>-7</sup>	[49]
EtOH/HEPES buffer (95/5)	/	/	/	5.03 × 10 <sup>-7</sup>	[50]
methanol	2.54 × 10 <sup>-9</sup>	4.23 × 10 <sup>-8</sup>	2.46 × 10 <sup>-9</sup>	/	This work
EtOH/H <sub>2</sub> O (15/1)	/	/	/	1.45 × 10 <sup>-7</sup>	

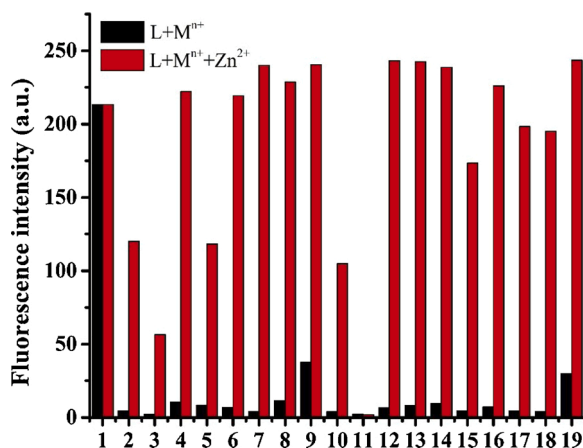


**Fig. 10.** Fluorescence response of L and L+Zn<sup>2+</sup> upon the addition of various metal.

ions (1=Zn<sup>2+</sup>, 2=Fe<sup>2+</sup>, 3=Fe<sup>3+</sup>, 4=Ag<sup>+</sup>, 5=Al<sup>3+</sup>, 6=Ba<sup>2+</sup>, 7=Co<sup>2+</sup>, 8=Ca<sup>2+</sup>, 9=Cd<sup>2+</sup>, 10=Cr<sup>3+</sup>, 11=Cu<sup>2+</sup>, 12=Hg<sup>2+</sup>, 13=K<sup>+</sup>, 14=Li<sup>+</sup>, 15=Mn<sup>2+</sup>, 16=Na<sup>+</sup>, 17=Ni<sup>+</sup>, 18= Pb<sup>2+</sup>, 19=Mg<sup>2+</sup>) in EtOH/H<sub>2</sub>O (15/1, V/V).

studies of L to Zn<sup>2+</sup> were conducted in EtOH/H<sub>2</sub>O (15/1, V/V). The UV–vis titration of L to M<sup>3+</sup> took Al<sup>3+</sup> as an example. As shown in Fig. 1, the single probe L had absorption at 287 nm and 325 nm. After Al<sup>3+</sup> was added, the absorption appeared at 505 nm. And with the gradual addition of Al<sup>3+</sup>, the absorption peak at 505 nm gradually increased, and the absorption peak at 325 nm gradually decreased. And it could be observed that an isosbestic point appeared at 345 nm. These changes indicated that an interaction took place between L and Al<sup>3+</sup>. The UV–vis titration spectra of L to Fe<sup>3+</sup> and L to Cr<sup>3+</sup> were shown in Figs. S9 and S10, respectively. The UV–vis titration of L to Zn<sup>2+</sup> was expressed in Fig. 2. The absorption peak of L alone had absorption at 287 nm and 325 nm. After Zn<sup>2+</sup> was added, the absorption appeared at 405 nm, 425 nm and 455 nm. And with the gradually adding of Zn<sup>2+</sup>, the absorption peaks at 405 nm, 425 nm, and 455 nm gradually increased, and the absorption peaks at 325 nm gradually decreased. And an isosbestic point could be observed at 355 nm. Similarly, these changes indicated that an interaction took place between L and Zn<sup>2+</sup>.

### 3.2. Effect of solvent

To explore the effect of solvent on the selectivity of L to M<sup>3+</sup> and L to Zn<sup>2+</sup>, fluorescence experiments of L to M<sup>3+</sup> and L to Zn<sup>2+</sup> in different solvents were carried out. Firstly, when the excitation wavelength was set to 490 nm, the L after addition of Al<sup>3+</sup> was subjected to fluorescence detection in ethanol, methanol, acetonitrile, ethyl acetate, dichloromethane, DMSO and DMF. As shown in Fig. 3, the L-Al<sup>3+</sup> system showed the strongest fluorescence in methanol solvent. However, under the condition of an excitation wavelength of 425 nm, L after adding Cd<sup>2+</sup>, Zn<sup>2+</sup>, Mg<sup>2+</sup> respectively exhibited fluorescence in ethanol solution (Fig. 4a). We tried to change the fluorescence intensity of L after adding

metal ions by adjusting the polarity of the solvent [39]. We first adjusted the ratio of ethanol to water as 20:1, as shown in Fig. 4b, although the fluorescence intensity of L after adding Mg<sup>2+</sup> or Cd<sup>2+</sup> was reduced, it still interfered with the detection of Zn<sup>2+</sup>. We continued to increase the proportion of water and set the ratio of ethanol to water as 10:1 (Fig. 4c). At this time, not only the fluorescence of L-Mg<sup>2+</sup> and L-Cd<sup>2+</sup> were significantly quenched, but the fluorescence intensity of L-Zn<sup>2+</sup> was also reduced obviously. Therefore, we adjusted the EtOH/H<sub>2</sub>O as 15:1. In this solution, Mg<sup>2+</sup> and Cd<sup>2+</sup> have almost no interference in detecting Zn<sup>2+</sup>. This indicated that L had good selectivity for the detection of Zn<sup>2+</sup> in EtOH/H<sub>2</sub>O (15/1, V/V).

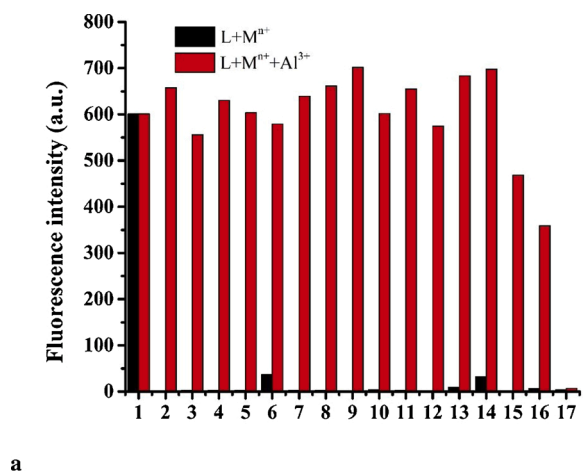
### 3.3. Effect of pH

In order to detect metal ions in various environments, it is important to determine the pH range where the probe emits the best fluorescence. Since the pH could not be adjusted in pure methanol solvent, we studied whether the pH value affected the fluorescence emission of L and L-Zn<sup>2+</sup> complexes in HEPES buffer. The ideal pH condition for the best fluorescence emission was determined when the probe L was combined with Zn<sup>2+</sup>. The effect of pH on the emission intensity of L and L-Zn<sup>2+</sup> complexes were monitored in the pH range of 1–14 (Fig. 5). The fluorescence emission intensity of probe L was basically not affected by the pH value, and the fluorescence intensity of L-Zn<sup>2+</sup> was the strongest only when the pH was 7. The fluorescence intensity of L-Zn<sup>2+</sup> at other pH values was basically the same as that of L. From this, we could infer that L did not coordinate with Zn<sup>2+</sup> in other pH environments. The results of the pH range demonstrated that the probe L was suitable for the detection of Zn<sup>2+</sup> in a pH = 7 environment.

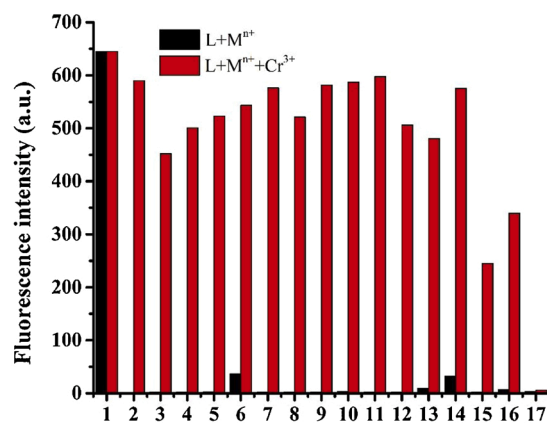
### 3.4. Selectivity of L to Zn<sup>2+</sup> and M<sup>3+</sup>

Fluorescence spectra analysis experiments were carried out to research the selective recognition of metal ions by the probe L. As depicted in Fig. 6, in EtOH/H<sub>2</sub>O (15/1, V/V) solution, L alone was no obvious fluorescence emission at 498 nm when the excitation wavelength was set at 425 nm. However, after addition of Zn<sup>2+</sup>, the significant fluorescence emission at 498 nm was observed. In addition, after adding other metal ions, there was only weak or almost no fluorescence emission. It was worth mentioning that when Cu<sup>2+</sup> was added, the EtOH/H<sub>2</sub>O (15/1, V/V) solution of L showed a red color which was different from other metal ions. In addition, after Al<sup>3+</sup>, Fe<sup>3+</sup>, and Cr<sup>3+</sup> were added to L, they appeared pink color with faint pink fluorescence at 588 nm.

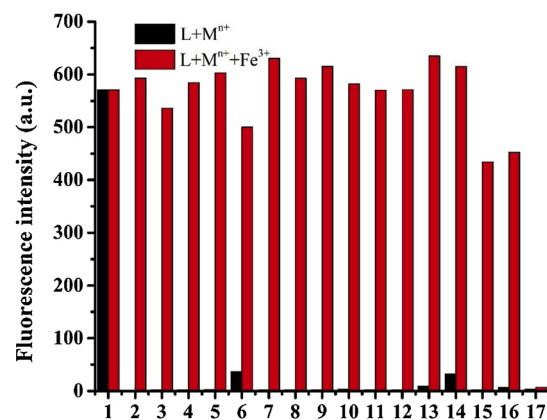
The selective fluorescence response experiment of L to M<sup>3+</sup> was carried out in methanol solution. Fig. 7 showed the fluorescence response spectrum of probe L to M<sup>3+</sup> when the excitation wavelength was set to 490 nm. L alone showed no fluorescence and the color of the solution was colorless. When M<sup>3+</sup> was added to the methanol solution of L, the solution appeared pink, at the same time, the methanol solution of L with M<sup>3+</sup> showed obvious fluorescence emission at 588 nm. Except for the L solution containing Zn<sup>2+</sup> and Co<sup>2+</sup>, which performed weak fluorescence, all other metal ions had no apparent fluorescence. Therefore, L



a



b



c

**Fig. 11.** a. Fluorescence response of L and L+Al<sup>3+</sup> upon the addition of various metal ions (1=Al<sup>3+</sup>, 2=Ag<sup>+</sup>, 3=Ba<sup>2+</sup>, 4=Ca<sup>2+</sup>, 5=Cd<sup>2+</sup>, 6=Co<sup>2+</sup>, 7=Hg<sup>2+</sup>, 8=K<sup>+</sup>, 9=Li<sup>+</sup>, 10=Mg<sup>2+</sup>, 11=Mn<sup>2+</sup>, 12=Na<sup>+</sup>, 13=Pb<sup>2+</sup>, 14=Zn<sup>2+</sup>, 15=Fe<sup>2+</sup>, 16=Ni<sup>2+</sup>, 17=Cu<sup>2+</sup>) in methanol. b. Fluorescence response of L and L+Cr<sup>3+</sup> upon the addition of various metal ions (1=Cr<sup>3+</sup>, 2=Ag<sup>+</sup>, 3=Ba<sup>2+</sup>, 4=Ca<sup>2+</sup>, 5=Cd<sup>2+</sup>, 6=Co<sup>2+</sup>, 7=Hg<sup>2+</sup>, 8=K<sup>+</sup>, 9=Li<sup>+</sup>, 10=Mg<sup>2+</sup>, 11=Mn<sup>2+</sup>, 12=Na<sup>+</sup>, 13=Pb<sup>2+</sup>, 14=Zn<sup>2+</sup>, 15=Fe<sup>2+</sup>, 16=Ni<sup>2+</sup>, 17=Cu<sup>2+</sup>) in methanol. c. Fluorescence response of L and L+Fe<sup>3+</sup> upon the addition of various metal ions (1=Fe<sup>3+</sup>, 2=Ag<sup>+</sup>, 3=Ba<sup>2+</sup>, 4=Ca<sup>2+</sup>, 5=Cd<sup>2+</sup>, 6=Co<sup>2+</sup>, 7=Hg<sup>2+</sup>, 8=K<sup>+</sup>, 9=Li<sup>+</sup>, 10=Mg<sup>2+</sup>, 11=Mn<sup>2+</sup>, 12=Na<sup>+</sup>, 13=Pb<sup>2+</sup>, 14=Zn<sup>2+</sup>, 15=Fe<sup>2+</sup>, 16=Ni<sup>2+</sup>, 17=Cu<sup>2+</sup>) in methanol.

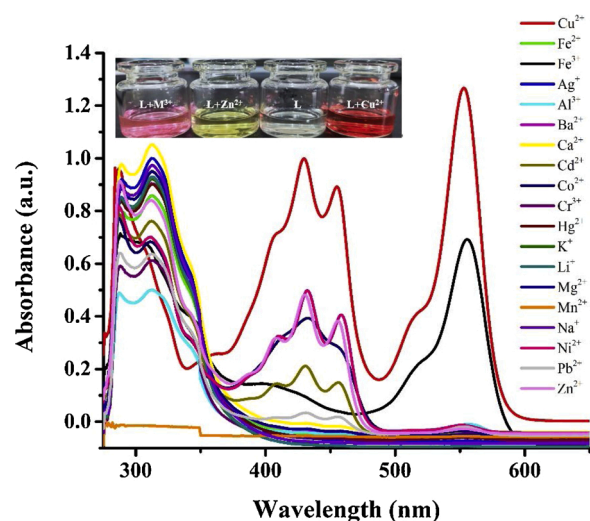


**Fig. 12.** The UV-vis absorption spectra of L after addition of 1 equiv of various metal ions in EtOH/H<sub>2</sub>O (15/1, V/V). Inset: Color changes of probe L and L in the presence of Cu<sup>2+</sup>, Zn<sup>2+</sup> and M<sup>3+</sup> under sunlight.

showed more selective to M<sup>3+</sup> (excited at 490 nm) than other monovalent and divalent metal cations in methanol.

### 3.5. Titration experiment of L to M<sup>3+</sup> and Zn<sup>2+</sup>

The fluorescence titration experiments were conducted to explore the relationship between fluorescence intensity and metal ion concentration. Fig. 8 was the fluorescence titration spectrum of L in EtOH/H<sub>2</sub>O (15/1, V/V) solution with continuous dropwise addition of Zn<sup>2+</sup> (0.0–1.1 equiv). It could be seen intuitively from the spectrum that as the concentration of Zn<sup>2+</sup> increased, the fluorescence intensity at 498 nm enhanced gradually. When Zn<sup>2+</sup> was added to 1.0 equiv, the fluorescence intensity was basically stable, indicating that the L-Zn<sup>2+</sup> compound with a coordination ratio of 1:1 had been formed. Besides, the fluorescence intensity had a linear relationship with Zn<sup>2+</sup> (Fig. S4). According to the formula  $LOD = 3\sigma/k$ , the detection limit of L for Zn<sup>2+</sup> was calculated to be  $1.45 \times 10^{-7}$  M. The binding constant ( $K_a$ ) of L and Zn<sup>2+</sup> calculated by the Benesi-Hildebrand equation was  $6.75 \times 10^4$  M<sup>-1</sup> (Fig. S5).

$$\frac{1}{F - F_{\min}} = \frac{1}{K_a(F_{\max} - F_{\min})[Zn^{2+}]} + \frac{1}{F_{\max} - F_{\min}}$$

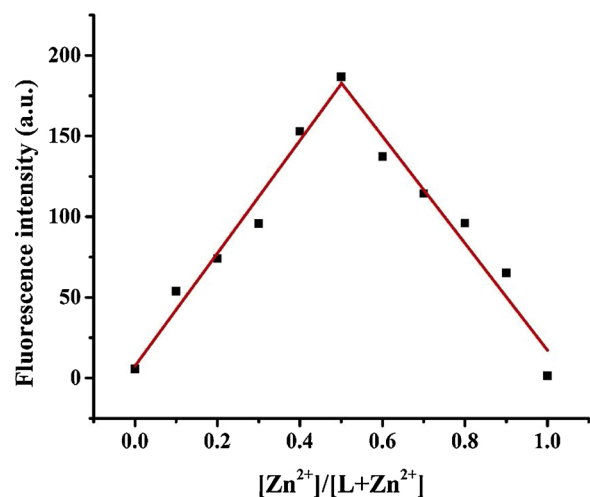


**Fig. 13.** Job's plot for determining the stoichiometry between L and Zn<sup>2+</sup> in EtOH/H<sub>2</sub>O (15/1, V/V).

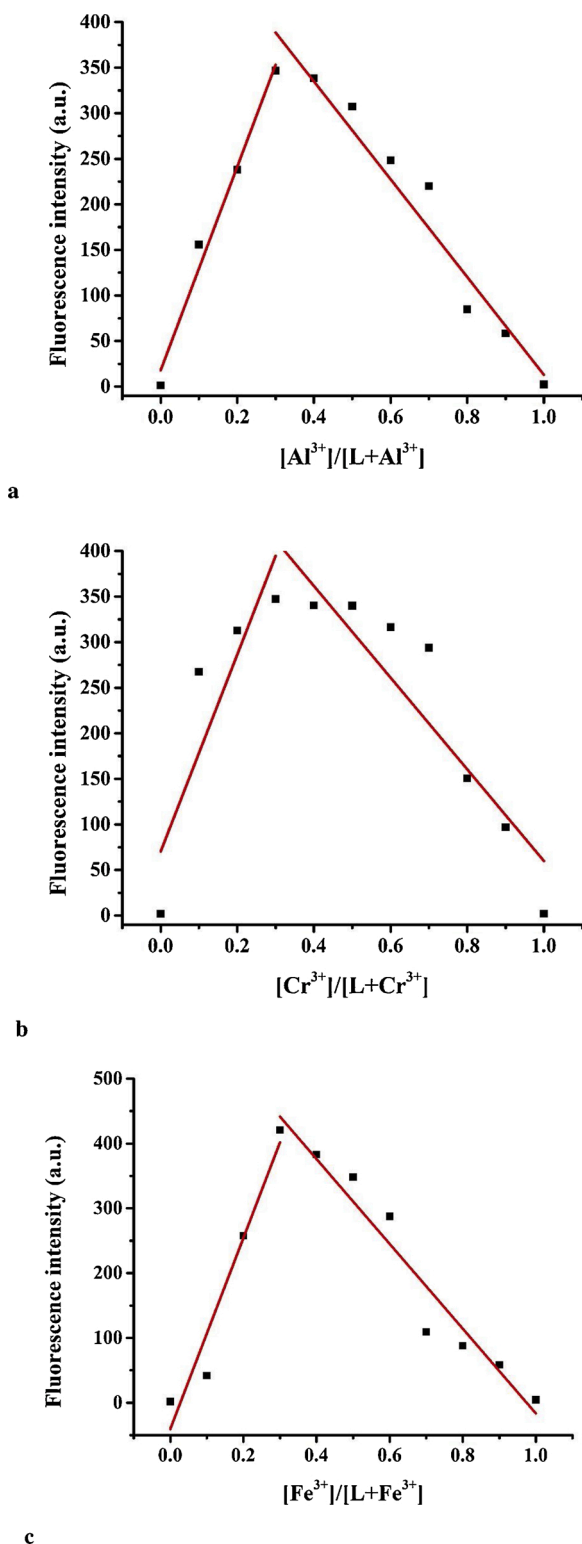


**Fig. 14.** a. Job's plot for determining the stoichiometry between L and  $\text{Al}^{3+}$  in methanol. b. Job's plot for determining the stoichiometry between L and  $\text{Cr}^{3+}$  in methanol. c. Job's plot for determining the stoichiometry between L and  $\text{Fe}^{3+}$  in methanol.

Herein,  $F_{\text{max}}$ ,  $F_{\text{min}}$  and  $F$  respectively indicated the fluorescence intensity (emission wavelength was 498 nm) of the maximum concentration of  $\text{Zn}^{2+}$ , L alone, and the various concentration of  $\text{Zn}^{2+}$ .

Similarly, the fluorescence titration experiments of L to  $\text{M}^{3+}$  were carried out according to the above method. As demonstrated in Fig. 9, as

$\text{M}^{3+}$  was gradually added, the wavelength was gradually redshifted from 580 nm to 588 nm and the fluorescence intensity at 588 nm increased gradually. When  $\text{M}^{3+}$  was dropped to 0.5 equiv, the fluorescence intensity remained basically unchanged, which indicated that the  $\text{L-M}^{3+}$  complex had been formed this moment. The linear relationship between metal ion concentration and fluorescence emission intensity was also fitted (Fig. S6). The detection limits of L for  $\text{Fe}^{3+}$ ,  $\text{Al}^{3+}$  and  $\text{Cr}^{3+}$  were  $2.46 \times 10^{-9}$  M,  $2.54 \times 10^{-9}$  M and  $4.23 \times 10^{-8}$  M, respectively. According to the Benesi-Hildebrand equation, the binding constants between L and  $\text{Fe}^{3+}$ , between L and  $\text{Al}^{3+}$ , and between L and  $\text{Cr}^{3+}$  were  $4.23 \times 10^5$   $\text{M}^{-1}$ ,  $2.41 \times 10^5$   $\text{M}^{-1}$  and  $3.93 \times 10^5$   $\text{M}^{-1}$ , respectively (Fig. S7). We compared the probe we synthesized with the  $\text{M}^{3+}$  and  $\text{Zn}^{2+}$  probe previously reported (Table 1), the probe in our work had a lower detection limit and could be used as a dual detection probe for  $\text{M}^{3+}$  and  $\text{Zn}^{2+}$ .

### 3.6. Competitive experiment of L to $\text{Zn}^{2+}$ and L to $\text{M}^{3+}$

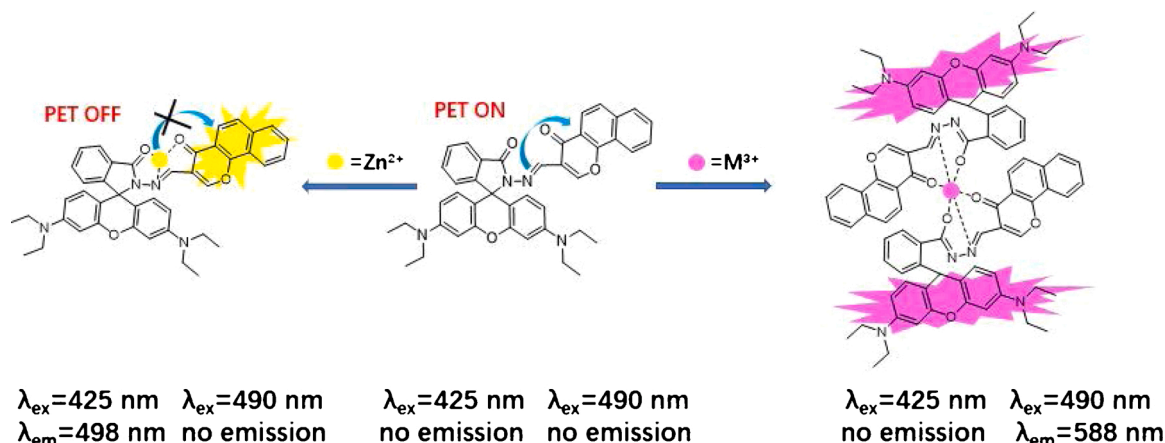
To further explore the selectivity of L to  $\text{Zn}^{2+}$  in the presence of other metal ions such as  $\text{Na}^+$ ,  $\text{Mg}^{2+}$ ,  $\text{Ag}^+$ ,  $\text{K}^+$ ,  $\text{Li}^+$ ,  $\text{Hg}^{2+}$ ,  $\text{Cu}^{2+}$ ,  $\text{Ca}^{2+}$ ,  $\text{Co}^{2+}$ ,  $\text{Cd}^{2+}$ ,  $\text{Mn}^{2+}$ ,  $\text{Ba}^{2+}$ ,  $\text{Pb}^{2+}$ ,  $\text{Al}^{3+}$ ,  $\text{Cr}^{3+}$  and  $\text{Fe}^{3+}$ , fluorescence analysis experiments were carried out. The results were illustrated in Fig. 10, when  $\text{Zn}^{2+}$  was added to L with addition of other metal ions, except for  $\text{Cu}^{2+}$ , other metal ions showed fluorescence emission, which indicated those metal ions would not interfere the coordination of L and  $\text{Zn}^{2+}$ . This might be due to the paramagnetism of  $\text{Cu}^{2+}$ , which led to the transfer of electrons and energy from the ligand to the metal ion. When  $\text{Zn}^{2+}$  was added to  $\text{L-Cu}^{2+}$ , fluorescence quenching would occur. This result indicated that other metal ions would not interfere with the selectivity of L to  $\text{Zn}^{2+}$ . We used the same method to detect whether other metal ions would affect the coordination of  $\text{L-M}^{3+}$ . The spectrum was shown in Fig. 11, the result was similar to the above, except for  $\text{Cu}^{2+}$ , other metal ions would not interfere with  $\text{L-M}^{3+}$ . Similarly, other metal ions would not affect the selectivity of L to  $\text{M}^{3+}$ .

### 3.7. UV-vis spectroscopy experiment of L on $\text{Cu}^{2+}$

In EtOH/ $\text{H}_2\text{O}$  (15/1, V/V), it was found that L after adding  $\text{Cu}^{2+}$  showed a red color different from L after adding others. Therefore, the UV-vis spectrum analysis method was used to study the selectivity of L to  $\text{Cu}^{2+}$ . The UV-vis spectrum was shown in Fig. 12, L added with  $\text{Cu}^{2+}$  showed absorption band at 409 nm, 430 nm, 455 nm and 553 nm, while L after adding other metal ions were no absorption band except  $\text{M}^{3+}$ ,  $\text{Ni}^{2+}$ ,  $\text{Zn}^{2+}$ ,  $\text{Co}^{2+}$ ,  $\text{Cd}^{2+}$  and  $\text{Pb}^{2+}$ . Although L after adding  $\text{Fe}^{3+}$  showed a clear pink color and exhibited obvious absorption band at 553 nm, there was no absorption band at 409 nm, 430 nm, 455 nm, which would not affect the detection of  $\text{Cu}^{2+}$ . Similarly, the yellow-colored L with the addition of  $\text{Ni}^{2+}$ ,  $\text{Zn}^{2+}$ ,  $\text{Co}^{2+}$ ,  $\text{Cd}^{2+}$  and  $\text{Pb}^{2+}$  respectively had absorption bands at 409 nm, 430 nm, and 455 nm, but there was no absorption at 553 nm, and it would also not interfere with the selectivity of L to  $\text{Cu}^{2+}$ . This suggested that L had favorable recognition of  $\text{Cu}^{2+}$ . The change in wavelength was caused by the change in the color of the solution. The color change from colorless to red, which could be observed with the naked eye. Moreover, the competitive experiment of  $\text{L-Cu}^{2+}$  was carried out, and other metal ions would not interfere with the coordination of L and  $\text{Cu}^{2+}$  (Fig. S8).

### 3.8. Coordination studies

The Job's plot of  $\text{L-Zn}^{2+}$  was researched based on the fluorescence spectrum. The total concentration of L and specific metal ions kept constant (25  $\mu\text{M}$ ), and the molar fraction ratio was continuously variable ( $[\text{M}^{n+}]/([\text{L}]+[\text{M}^{n+}])$ ). As shown in Fig. 13, as the mole fraction was 0.5, the fluorescence intensity reached the maximum, which signified that the coordination ratio of L and  $\text{Zn}^{2+}$  was 1:1. Differently, in the Job's plot of  $\text{L-M}^{3+}$ , when the mole fraction was 0.3, the fluorescence intensity reached the maximum. The Job's plot of  $\text{L-M}^{3+}$  indicated that the



Scheme 2. The proposed sensing mechanism of **L** with  $\text{Zn}^{2+}$  and  $\text{M}^{3+}$ .

coordination ratio of **L** and  $\text{M}^{3+}$  was 2:1 (Fig. 14a–c).

### 3.9. The sensing mechanism of **L**

When **L** is present alone, the nitrogen atom of the hydrazide moiety of Rhodamine B transfers electrons to the moiety of 4-oxo-4H-benzo[h]methylene-3-carbaldehyde, causing the individual **L** to not show fluorescence, which is due to the light-induced electron transfer process (PET) [40–42]. When  $\text{Zn}^{2+}$  is added to **L**, the carbonyl oxygen atom of rhodamine B and the nitrogen atom in the  $-\text{C}=\text{N}-$  group coordinated with  $\text{Zn}^{2+}$ , PET was inhibited, and  $\text{L}-\text{Zn}^{2+}$  emitted fluorescence. For the coordination of **L** and  $\text{M}^{3+}$ , due to the ring opening of Rhodamine B spirolactam [43,44], when  $\text{M}^{3+}$  was added to **L**,  $\text{L}-\text{M}^{3+}$  exhibited strong fluorescence (Scheme 2).

## 4. Conclusion

In summary, the synthesis of fluorescent probe 7,8-benzochromone-3-carbaldehyde-(rhodamine B carbonyl) hydrazone (**L**) was reported. The probe showed a fluorescence response to trivalent ions ( $\text{Al}^{3+}$ ,  $\text{Fe}^{3+}$ ,  $\text{Cr}^{3+}$ ) in methanol solution when the excitation wavelength was 490 nm and the emission wavelength was 588 nm. In addition, the detection limits of **L** for  $\text{Fe}^{3+}$ ,  $\text{Al}^{3+}$  and  $\text{Cr}^{3+}$  were  $2.46 \times 10^{-9} \text{ M}$ ,  $2.54 \times 10^{-9} \text{ M}$  and  $4.23 \times 10^{-8} \text{ M}$ , respectively. More importantly, the probe **L** exhibited high selectivity towards  $\text{Zn}^{2+}$  ( $\lambda_{\text{ex}} = 425 \text{ nm}$ ,  $\lambda_{\text{em}} = 498 \text{ nm}$ ) in EtOH/ $\text{H}_2\text{O}$  (15/1, V/V). Besides, **L** addition with  $\text{Cu}^{2+}$  appeared red, which was different from **L** after the addition of other metal ions in this solution, indicating that **L** could be used as a colorimetric probe of  $\text{Cu}^{2+}$ .

### CRedit authorship contribution statement

**Jie Sun:** Conceptualization, Data curation, Formal analysis, Investigation, Software, Validation, Visualization, Writing - original draft, Writing - review & editing, Resources, Methodology. **Tian-rong Li:** Project administration, Supervision. **Zheng-yin Yang:** Project administration, Funding acquisition, Supervision.

### Declaration of Competing Interest

We have no conflicts of interest to declare.

### Acknowledgments

This work is supported by the National Natural Science Foundation of China (21761019).

## Appendix A. Supplementary data

Supplementary material related to this article can be found, in the online version, at doi:<https://doi.org/10.1016/j.jphotochem.2021.113207>.

## References

- [1] W. Cao, X.J. Zheng, J.P. Sun, W.T. Wong, D.C. Fang, J.X. Zhang, L.P. Jin, *Inorg. Chem.* 53 (2014) 3012–3021.
- [2] R.S. Kathayat, N.S. Finney, *J. Am. Chem. Soc.* 135 (2013) 12612–12614.
- [3] D. Jimenez, R. Martinez-Manez, F. Sancenon, J.V. Ros-Lis, A. Benito, J. Soto, *J. Am. Chem. Soc.* 125 (2003) 9000–9001.
- [4] P. Thirupathi, J.Y. Park, L.N. Neupane, M.Y.L.N. Kishore, K.-H. Lee, *ACS Appl. Mater. Inter.* 7 (2015) 14243–14253.
- [5] C. Kar, S. Samanta, S. Mukherjee, B.K. Datta, A. Ramesh, G. Das, *New J. Chem.* 38 (2014) 2660–2669.
- [6] J.C. Qin, Z.Y. Yang, L. Fan, X.Y. Cheng, T.R. Li, B.D. Wang, *Anal. Methods-UKs* 6 (2014) 7343–7348.
- [7] X. Liu, J.J. Xiang, Y. Tang, X.L. Zhang, Q.Q. Fu, J.H. Zou, Y.H. Lin, *Anal. Chim. Acta* 745 (2012) 99–105.
- [8] P. Saluja, H. Sharma, N. Kaur, N. Singh, D.O. Jang, *Tetrahedron* 68 (2012) 2289–2293.
- [9] P.H. Xie, F.Q. Guo, Y. Xiao, Q. Jin, D.H. Yao, Z.H. Huang, *J. Lumin.* 140 (2013) 45–50.
- [10] S. Samanta, S. Goswami, A. Ramesh, G. Das, *Sens. Actuators B-Chem.* 194 (2014) 120–126.
- [11] S.H. Ren, S.G. Liu, Y. Ling, Y. Shi, N.B. Li, H.Q. Luo, *Anal. Bioanal. Chem.* 411 (2019) 3301–3308.
- [12] D.A. Eastmond, J.T. MacGregor, R.S. Slesinski, *Crit. Rev. Toxicol.* 38 (2008) 173–190.
- [13] X.M. Li, R.R. Zhao, Y. Yang, X.W. Lv, Y.L. Wei, R. Tan, J.F. Zhang, Y. Zhou, *Chin. Chem. Lett.* 28 (2017) 1258–1261.
- [14] T. Rasheed, C. Li, M. Bilal, C. Yu, H.M.N. Iqbal, *Sci. Total Environ.* 640 (2018) 174–193.
- [15] P. Mahato, S. Saha, E. Suresh, R. Di Liddo, P.P. Parnigotto, M.T. Conconi, M. K. Kesharwani, B. Ganguly, A. Das, *Inorg. Chem.* 51 (2012) 1769–1777.
- [16] F.W. Wang, H.D. Duan, D.X. Xing, G. Yang, *J. Fluoresc.* 27 (2017) 1721–1727.
- [17] H. He, Y. Li, L.F. He, S. Afr. J. Bot. 123 (2019) 23–29.
- [18] S.G. Lambert, J.A.M. Taylor, K.L. Wegener, S.L. Woodhouse, S.F. Lincoln, A. D. Ward, *New J. Chem.* 24 (2000) 541–546.
- [19] D. Maity, T. Govindaraju, *Chem. Commun.* 46 (2010) 4499–4501.
- [20] Y.S. Jang, B. Yoon, J.M. Kim, *Macromol. Res.* 19 (2011) 97–99.
- [21] X. Tang, Y. Wang, J. Han, L. Ni, L. Wang, L.H. Li, H.Q. Zhang, C. Li, J. Li, H.R. Li, *Spectrochim. Acta A* 191 (2018) 172–179.
- [22] Y.M. Liu, J.Y. Zhang, J.X. Ru, X. Yao, Y. Yang, X.H. Li, X.L. Tang, G.L. Zhang, W. S. Liu, *Sens. Actuators B-Chem.* 237 (2016) 501–508.
- [23] M. Andjelkovic, J. Van Camp, B. De Meulenaer, G. Depaemelaere, C. Socaciu, M. Verloo, R. Verhe, *Food Chem.* 98 (2006) 23–31.
- [24] K.D. Welch, T.Z. Davis, S.D. Aust, *Arch. Biochem. Biophys.* 397 (2002) 360–369.
- [25] T. Ganz, *Blood* 102 (2003) 783–788.
- [26] W.H. Tang, Y. Tian, B.P. Li, Q.H. Liu, D.Q. Wang, X.F. Jing, J.J. Zhang, S.Q. Xu, *Spectrochim. Acta A* 210 (2019) 341–347.
- [27] L. Wang, X.D. Yang, X.L. Chen, Y.P. Zhou, X.D. Lu, C.G. Yan, Y.K. Xu, R.Y. Liu, J. Q. Qu, *Mater. Sci. Eng. C* 72 (2017) 551–557.
- [28] J.C. Duvaligneu, C. Piskernik, S. Haindl, B. Kloesch, R.T. Hartl, M. Huettemann, I. Lee, T. Ebel, R. Moldzio, M. Gemeiner, H. Redl, A.V. Kozlov, *Lab. Invest.* 88 (2008) 70–77.

- [29] G.T. Suck, Z.A. Yegin, Z.N. Oezkurt, S.Z. Aki, T. Karakan, G. Akyol, Bone. Marrow. Transpl. 42 (2008) 461–467.
- [30] S.H. Hou, Z.G. Qu, K.L. Zhong, Y.J. Bian, L.J. Tang, Tetrahedron Lett. 57 (2016) 2616–2619.
- [31] A. Barba-Bon, A.M. Costero, S. Gil, M. Parra, J. Soto, R. Martinez-Manez, F. Sancenon, Chem. Commun. 48 (2012) 3000–3002.
- [32] W.Y. Li, Z.C. Liu, B.Q. Fang, M. Jin, Y. Tian, Biosens. Bioelectron. 148 (2020), 111666.
- [33] N.A. Dudina, E.V. Antina, G.B. Guseva, A.I. Vyugin, J. Fluoresc. 24 (2014) 13–17.
- [34] S.N. Ansari, A.K. Saini, P. Kumari, S.M. Mobin, Inorg. Chem. Front. 6 (2019) 736–745.
- [35] J.X. Fu, Y.X. Chang, B. Li, H.H. Mei, K.X. Xu, Appl. Organomet. Chem. 33 (2019) e5162.
- [36] T.T. Kang, H.P. Wang, X.J. Wang, L.H. Feng, Microchem. J. 148 (2019) 442–448.
- [37] M. Jakubek, Z. Kejik, V. Parchansky, R. Kaplanek, L. Vasina, P. Martasek, V. Kral, Supramol. Chem. 29 (2017) 1–7.
- [38] X.L. Yue, C.R. Li, Z.Y. Yang, J. Photochem. Photobiol. A: Chem. 351 (2018) 1–7.
- [39] H.P. Wang, T.T. Kang, X.J. Wang, L.H. Feng, Talanta 184 (2018) 7–14.
- [40] W. Sun, M. Li, J.L. Fan, X.J. Peng, Acc. Chem. Res. 52 (2019) 2818–2831.
- [41] C.C. Du, S.B. Fu, X.H. Wang, A.C. Sedgwick, W. Zhen, M.J. Li, X.Q. Li, J. Zhou, Z. Wang, H.Y. Wang, J.L. Sessler, Chem. Sci. 10 (2019) 5699–5704.
- [42] D. Soni, N. Duvva, D. Badgurjar, T.K. Roy, S. Nimesh, G. Arya, L. Giribabu, R. Chitta, Chem.-Asian. J. 13 (2018) 1594–1608.
- [43] M. Beija, C.A.M. Afonso, J.M.G. Martinho, Chem. Soc. Rev. 38 (2009) 2410–2433.
- [44] K. Li, Y. Xiang, X.Y. Wang, J. Li, R.R. Hu, A.J. Tong, B.Z. Tang, J. Am. Chem. Soc. 136 (2014) 1643–1649.
- [45] S. Paul, A. Manna, S. Goswami, Dalton Trans. 44 (2015) 11805–11810.
- [46] S. Goswami, K. Aich, A.K. Das, A. Manna, S. Das, RSC Adv. 3 (2013) 2412–2416.
- [47] F. Ye, N. Wu, P. Li, Y.L. Liu, S.J. Li, Y. Fu, Spectrochim. Acta A 222 (2019), 117242.
- [48] L. Yan, X.Y. Wen, Z.F. Fan, Anal. Bioanal. Chem. 412 (2020) 1453–1463.
- [49] T.T. Liu, J. Xu, C.G. Liu, S. Zeng, Z.Y. Xing, X.J. Sun, J.L. Li, J. Mol. Liq. 300 (2020), 112250.
- [50] J.L. Zhu, Y.H. Zhang, Y.H. Chen, T.M. Sun, Y.F. Tang, Y. Huang, Q.Q. Yang, D. Y. Ma, Y.P. Wang, M. Wang, Tetrahedron Lett. 58 (2017) 365–370.